Journal of Organometallic Chemistry, 208 (1981) 55—71
Elsevier Sequoia S.A., Lausanne — Printed in The Netherlands

X-RAY DIFFRACTION STUDIES OF THE INFLUENCE OF LATTICE EFFECTS ON THE METAL CARBONYL FRAMEWORK OF THE $[Mo_2(CO)_{10}(\mu\text{-}H)]^-$ MONOANION

JEFFREY L. PETERSEN *, ALBERT MASINO

Department of Chemistry, West Virginia University, Morgantown, West Virginia 26506 (U.S.A.)

and ROBERT P. STEWART, Jr.

Department of Chemistry, Miami University, Oxford, Ohio 45056 (U.S.A.)

(Received August 5th, 1980)

Summary

X-ray diffraction studies of the $[Et_4N]^+$, $[(Ph_3P)_2N]^+$, and $[K(crypt\text{-}222)]^+$ salts of the $[Mo_2(CO)_{10}(\mu\text{-}H)]^-$ monoanion were undertaken to examine the influence of lattice effects upon the anion's solid-state geometry. The outcome of these studies has shown that the $[Mo_2(CO)_{10}(\mu\text{-}H)]^-$ anion can adopt either a linear, eclipsed ($[Et_4N]^+$ salt) or an appreciably bent, staggered ($[(Ph_3P)_2N]^+$ and $[K(crypt\text{-}222)]^+$ salts) configuration with the degree of bending dictated by the choice of the cation. For the fully characterized $[(Ph_3P)_2N]^+$ and $[K(crypt\text{-}222)]^+$ salts the corresponding dihedral angles between the two equatorial planes in the anion are 15.4° and 29.9°, respectively. This greater bending of the Mo—H—Mo bond and the metal carbonyl framework for the latter salts is accompanied by a reduction of the Mo···Mo separation in the three-center, two-electron bond from 3.4219(9) to 3.4056(5) Å and a greater displacement of the equatorial carbon atoms out of their equatorial plane. All three salts crystallize in the triclinic space group, $P\bar{1}$. $[Et_4N]^+[Mo_2(CO)_{10}(\mu\text{-}H)]^-$ is isomorphous with the previously characterized tungsten analogue, whereas the refined lattice parameters for $[(Ph_3P)_2N]^+[Mo_2(CO)_{10}(\mu\text{-}H)]^-$ are a = 11.431(4), b = 14.267(4), c = 15.260(5) Å, α = 69.40(2), β = 88.03(3), γ = 80.18(2)° and for $[K(crypt\text{-}222)]^+$ $[Mo_2(CO)_{10}(\mu\text{-}H]^-$ are a = 10.056(2), b = 12.695(4), c = 15.946(5) Å, α = 71.56(2), β = 88.78(2), and γ = 86.16(2)°. Full-matrix least-squares refinement of the diffractometry data (with contributions included for all hydrogen atoms) led to final discrepancy indices of $R(F_o^2)$ = 0.045 and 0.035 for the $[(Ph_3P)_2N]^+$ and $[K(crypt\text{-}222)]^+$ salts, respectively.

0022—328X/81/0000—0000/$02.50,

Introduction

The stereochemistry and chemical reactivity of the $[M_2(CO)_{10}(\mu\text{-}H)]^-$ anion (M = Cr, Mo, W) have been studied extensively during the past several years. From a structural point of view, these compounds are of particular interest due to the presence of an unsupported three-center, two-electron M—H—M bond. Structural studies of various salts of the corresponding Cr [1—3] and W [4,5] compounds have shown that the solid state geometry of the anion can adopt several different configurations. Because of the apparent flexibility of the M—H—M linkage in $[M_2(CO)_{10}(\mu\text{-}H)]^-$, its metal carbonyl framework may vary from a linear, eclipsed configuration, such as observed for $[(Ph_3P)_2N]^+$-$[Cr_2(CO)_{10}(\mu\text{-}H)]^-$ [2b], to an appreciably bent, staggered configuration for the $[Ph_4P]^+$ [5] and $[(Ph_3P)_2N]^+$ [4] salts of $[W_2(CO)_{10}(\mu\text{-}H)]^-$. Although these structural variations may be attributed largely to lattice packing forces, our structural analysis of $[K(crypt\text{-}222)]^+[Cr_2(CO)_{10}(\mu\text{-}H)]^-$ [3] suggests that cation—anion interactions may also have a significant influence upon the anion's structure.

Despite the appreciable amount of structural information available for the Cr and W carbonylates, the solid state structure of the $[Mo_2(CO)_{10}(\mu\text{-}H)]^-$ anion has not been fully characterized. Darensbourg, Atwood, and coworkers [6,7], however, have studied phosphine substitution reactions and their mechanisms for $[Mo_2(CO)_{10}(\mu\text{-}H)]^-$. Their efforts have led to the isolation and structural characterization of both a monosubstituted hydride, $[Et_4N]^+[Mo_2(CO)_9(PPh_3)$-$(\mu\text{-}H)]^-$ [6], and a disubstituted species, $[Et_4N]^+[Mo_2(CO)_8(PMePh_2)_2(\mu\text{-}H)]^-$ [7]. Both binuclear anions possess a bent, staggered configuration with the phosphine substituent(s) residing *cis* to the hydride bridge. The disubstituted anion exhibits a greater bending of the molecular framework as evidenced by the angle of intersection defined by the two Mo—$CO_{(ax)}$ vectors of 148° for $[Mo_2(CO)_8(PMePh_2)_2(\mu\text{-}H)]^-$ compared to 163° for $[Mo_2(CO)_9(PPh_3)(\mu\text{-}H)]^-$. Although this structural difference may be primarily due to a combination of steric and electronic effects, the importance of packing effects upon the solid-state structure of these hydride anions must also be considered. To provide the structural data necessary to evaluate the influence of lattice effects on the geometry of $[Mo_2(CO)_{10}(\mu\text{-}H)]^-$, we have undertaken X-ray diffraction studies of several salts of the unsubstituted molybdenum hydride anion. Details of the structure determinations for $[(Ph_3P)_2N]^+[Mo_2(CO)_{10}(\mu\text{-}H)]^-$ and $[K(crypt\text{-}222)]^+[Mo_2(CO)_{10}(\mu\text{-}H)]^-$ are discussed. The results of these studies complete the structural data base for this series of Group VIB hydrides and thereby provide an opportunity to examine the structural changes that accompany phosphine displacement of CO on $[Mo_2(CO)_{10}(\mu\text{-}H)]^-$.

Experimental

All syntheses were performed under a dry nitrogen atmosphere using solvents freshly distilled under N_2 or Ar prior to use and purified by standard methods. The $Mo(CO)_6$ and bis(triphenylphosphine)iminium chloride were purchased from Strem Chemical Company; KBH_4 and crypt-222, $C_{18}H_{36}N_2O_6$, were obtained from PCR, Inc. The infrared spectra were recorded on a Beckman IR-8

spectrometer using matched CaF_2 cells. Proton NMR spectra (THF-d_6) were measured on a Varian CFT-20 spectrometer operating in the FT mode. TMS was used as the internal standard. Microanalyses were performed by Galbraith Laboratories, Inc., Knoxville, Tennessee.

Preparation of salts of $[Mo_2(CO)_{10}(\mu\text{-}H)]^-$

The $[Et_4N]^+$, $[(Ph_3P)_2N]^+$, and $[K(crypt\text{-}222)]^+$ salts of $[Mo_2(CO)_{10}(\mu\text{-}H)]^-$ were prepared using published methods [8]. Samples suitable for chemical and structural analyses were recrystallized from THF/hexane or ethanol.

$[Et_4N]^+[Mo_2(CO)_{10}(\mu\text{-}H)]^-$. Anal. Found: C, 35.09; H, 3.71. Calcd. for $C_{18}H_{21}NO_{10}Mo_2$: C, 35.84; H, 3.51% IR ν(CO) (THF): 2043w, 1944s, 1880m. ^{1}H NMR spectrum: τ 6.72 (—CH_2—, quartet, J(H—H) = 10 Hz); τ 8.70 (—CH_3, triplet of triplets, J(H—H) = 10 Hz, J(N—CH_3) = 1.9 Hz); τ 22.14 (Mo—H, singlet). Rough lattice parameters for the reduced triclinic unit cell: a = 6.91, b = 8.94, c = 10.43 Å, α = 77.2, β = 86.7, γ = 77.9°.

$[(Ph_3P)_2N]^+[Mo_2(CO)_{10}(\mu\text{-}H)]^-$. Anal. Found: C, 54.48; H, 3.16. Calcd. for $C_{46}H_{31}NO_{10}P_2Mo_2$: C, 54.62; H, 3.09%. IR ν(CO) (THF): 2047w, 1946s, 1882m. ^{1}H NMR spectrum: τ 2.52 (—C_6H_5, complex multiplet), τ 22.15 (Mo—H, singlet).

$[K(crypt\text{-}222)]^+[Mo_2(CO)_{10}(\mu\text{-}H)]^-$. Anal. Found: C, 37.62; H, 4.44. Calcd. for $C_{28}H_{37}N_2O_{16}KMo_2$: 37.85; H, 4.20%. IR ν(CO) (THF): 2043w, 1944s. 1881m. ^{1}H NMR spectrum: τ 6.42 (—OCH_2CH_2O—, singlet); τ 6.46 (—OCH_2—, triplet, J(H—H) = 6 Hz); τ 7.45 (—CH_2N—, triplet, J(H—H) = 6 Hz); τ 22.15 (Mo—H, singlet).

Single-crystal X-ray diffraction data and data collection

A preliminary X-ray diffraction analysis of $[Et_4N]^+[Mo_2(CO)_{10}(\mu\text{-}H)]^-$ indicated that its crystal lattice is isomorphous with that for the Cr and W analogues. Consequently, diffractometry data were measured for only the $[(Ph_3P)_2N]^+$ and $[K(crypt\text{-}222)]^+$ salts.

The same general procedure was employed to collect the X-ray diffraction data for $[(Ph_3P)_2N]^+[Mo_2(CO)_{10}(\mu\text{-}H)]^-$ and $[K(crypt\text{-}222)]^+[Mo_2(CO)_{10}(\mu\text{-}H)]^-$. Preliminary oscillation and Weissenberg photographs of the crystalline samples were taken with Cu-K_α radiation and indicated the Laue symmetry to be C_i-$\bar{1}$. The ultimate structure in each case supported the selection of $P\bar{1}$ (C_i^1, No. 2) as the correct space group.

Each crystal was mounted on the end of a thin-glass fiber such that the crystal growth axis was nearly parallel to the spindle axis of the goniometer. The samples were protected from air and moisture by a thin-coating of a quick-drying shellac and then transferred to a Picker goniostat under computer control by a Krisel control diffractometer automation system. A peak search for low-angle reflections produced a sufficient number of reflections for the autoindexing routine *. The angular coordinates (ω, χ, and 2θ) of 20 higher order reflections were calculated, optimized by the automatic peak centering algorithm **, and least-squares fit to give the corresponding refined lattice parameters in Table 1 and the orientation matrix.

---

* The automatic indexing algorithm is based upon Jacobson's procedure [9].

** The automatic peak centering algorithm is similar to that described by Busing [10].

Intensity data (hkl, $h\bar{k}l$, $hk\bar{l}$, $h\bar{k}\bar{l}$) were measured with Zr-filtered Mo-K_α X-ray radiation (($K_{\alpha 1}$) 0.70926 Å, ($K_{\alpha 2}$) 0.71354 Å) at a take-off angle of 2°. The θ—2θ scan mode was employed with a fixed scan rate of 2.0°/min and variable scan widths calculated from the expression $w = A + B \tan \theta$. Background counts of 10 s duration were measured at the extremes of each scan using the (stationary-crystal)-(stationary-counter) method. The counter aperture of 1.0 mm diameter was placed 12 mm from the crystal. A scintillation counter was employed with the pulse height analyzer adjusted to accept 90% of the diffraction peak. During data collection the intensities of two standard reflections were measured periodically. The integrated intensity, I, and its standard deviation, $\sigma_c(I)$, for each of the measured peaks were calculated from the expressions $I = w(S/t_s - B/t_b)$ and $\sigma_c(I) = w(S/t_s^2 + B/t_b^2)^{1/2}$. In these equations S represents the total scan count measured in time t_s and B is the combined back-

TABLE 1

DATA FOR THE X-RAY DIFFRACTION ANALYSES OF THE $[(Ph_3P)_2N]^+$ AND $[K(crypt\text{-}222]^+$ SALTS OF $[Mo_2(CO)_{10}(\mu\text{-}H)]^-$

	$[(Ph_3P)_2N]^+$ Salt	$[K(crypt\text{-}222)]^+$ Salt
(A) Crystal data		
Crystal system	triclinic	triclinic
Space group	$P1(C_i^1$, no. 2)	$P\bar{1}(C_i^1$, No. 2)
a (Å)	11.431(4)	10.056(2)
b (Å)	14.267(4)	12.695(4)
c (Å)	15.260(5)	15.946(5)
α (°)	69.40(2)	71.56(2)
β (°)	88.03(3)	88.78(2)
γ (°)	80.18(2)	86.16(2)
volume (Å^3)	2295(1)	1927(1)
formula wt. (amu)	1011.58	888.58
density (obsd) (g cm^{-3})	1.43	1.52
density (calcd) (g cm^{-3})	1.464	1.531
Z, formula units/unit cell	2	2
μ (cm^{-1})	6.6	8.2
(B) Data collection and analysis summary		
crystal dimensions (mm)	0.27 × 0.20 × 0.40	0.175 × 0.23 × 0.33
detector angle range (°)	$5 < 2\theta < 40$	$5 < 2\theta < 45$
2θ-range for centered reflections (°)	25—32	25—34
scan-width parameters	$A = 1.6$; $B = 0.7$	A = 1.1; B = 0.8
no. of standard reflections	2(5 — 5 0. 5 4 6)	2(—2 4 5; 6 3 3)
crystal decay (%)	29	13
total no. of measured reflections	4589	5489
unique data used	3306 ($F_0^2 > 3\sigma(F_0^2)$)	3991 ($F_0^2 > \sigma(F_0^2)$)
agreement between equivalent data:		
$R_{av}(F_0)$	0.014	0.009
$R_{av}(F_0^2)$	0.010	0.010
transmission coefficients	0.87—0.90	0.83—0.87
p	0.04	0.03
$R(F_0)$	0.032	0.025
$R(F_0^2)$	0.045	0.035
$R_w(F_0^2)$	0.079	0.060
σ_1, error in observation of unit weight	1.57	1.38
no. of variables	550	442

ground count in time t_b. The intensity data were corrected for crystal decay, absorption and Lorentz-polarization effects. The unusually large intensity decay observed during the collection of the X-ray diffraction data for the $[(Ph_3P)_2N]^+$ salt was essentially linear with exposure time. The standard deviation of the square of each structure factor, $F_o^2 = AI/Lp$, was calculated from $\sigma(F_o^2) = [\sigma_c(F_o^2)^2 + (pF_o^2)^2]^{1/2}$. Duplicate reflections were averaged. No corrections for extinction were necessary. Additional details about the data collection procedure are summarized in Table 1.

Structural analysis

The crystal structure of $[(Ph_3P)_2N]^+[Mo_2(CO)_{10}(\mu\text{-H})]^-$ was determined by heavy-atom methods. The initial positions of the two independent Mo atoms were interpreted from the strongest peaks of an unsharpened three-dimensional Patterson map and used in subsequent Fourier summations to locate the remaining non-hydrogen atoms. Idealized positions for the phenyl hydrogens were calculated using MIRAGE [11]. A difference Fourier map calculated with low angle data ($\sin\theta/\lambda < 0.40$ A^{-1}) provided sufficient residual density to approximate the position of the bridging hydrogen atom in the anion. Its position was partially refined by varying it with only the positional and thermal parameters for the anion prior to the final refinement. Full-matrix least-squares refinement with anisotropic temperature factors for the 61 non-hydrogen atoms and fixed atom contributions for the 31 hydrogen atoms led to the final discrepancy indices of $R(F_o) = 0.032$, $R(F_o^2) = 0.045$, and $R_w(F_o^2) = 0.079$ with $\sigma_1 = 1.57$ for the 3306 reflections with $F_o^2 \geq 3\sigma(F_o^2)$.

The crystal structure of $[K(crypt\text{-}222)]^+[Mo_2(CO)_{10}(\mu\text{-H})]^-$ was solved with the aid of MULTAN 78 [12]. The approximate positions of the Mo atoms were initially interpreted from the first E-map calculated on the basis of the phase assignments for the noncentrosymmetric $P1$ space group. The coordinates of the actual center of symmetry were calculated and subtracted from the initial Mo positions to determine the approximate positions of the two independent Mo atoms in the centrosymmetric $P\bar{1}$ cell. Subsequent Fourier syntheses provided the coordinates for the remaining non-hydrogen atoms. Anisotropic thermal parameters were introduced and refined. A difference Fourier synthesis using only low angle data ($\sin\theta/\lambda < 0.40$ A^{-1}) led to the unambiguous location of all hydrogen atoms in the structure. The residual assigned to the bridging H atom corresponded to the largest peak on the difference Fourier map. Full-matrix least-squares refinement with anisotropic temperature factors for the 49 non-hydrogen atoms and fixed atom contributions for the 37 hydrogen atoms led to the final convergence with $R(F_o) = 0.025$, $R(F_o^2) = 0.035$, $R_w(F_o^2) = 0.060$, and $\sigma_1 = 1.38$ for 3991 reflections with $F_o^2 > \sigma(F_o^2)$.

The least-squares refinements of the X-ray diffraction data for both salts were based on the minimization of $\Sigma\omega_i|F_o^2 - S^2F_c^2|$ where the individual weight, ω_i, is equal to $1/\sigma^2(F_o^2)$ and S is the scale factor. The discrepancy indices were calculated from the expressions

$$R(F_o) = [\Sigma||F_o| - |F_c||/\Sigma|F_o|] ,$$

$$R(F_o^2) = \Sigma|F_o^2 - F_c^2|/\Sigma F_o^2 , \text{ and}$$

$$R_w(F_o^2) = [\Sigma\omega_i|F_o^2 - F_c^2|^2/\Sigma\omega_i F_o^4]^{1/2}$$

(Continued on p. 66)

TABLE 2

POSITIONAL PARAMETERS AND TEMPERATURE FACTORS FOR $[(Ph_3P)_2N]^+[Mo_2(CO)_{10}(\mu_2\text{-}H)]^-$ [a, b]

	Positional parameters			Temperature factors					
Atom	x	y	z	U_{11}	U_{22}	U_{33}	U_{12}	U_{13}	U_{23}
Mo(1)	0.06217(5)	0.27210(3)	0.20788(3)	968(4)	568(3)	718(3)	6(3)	−111(3)	−245(2)
Mo(2)	0.20016(4)	0.40221(3)	0.31205(3)	847(4)	584(3)	683(3)	−32(3)	−52(3)	−187(2)
C(1)	0.1058(6)	0.3735(5)	0.0837(5)	1147(55)	880(47)	992(51)	24(42)	−128(45)	−191(39)
C(2)	−0.1047(7)	0.3494(5)	0.1996(4)	1133(57)	903(46)	936(45)	105(43)	−87(44)	−465(37)
C(3)	0.0314(7)	0.1718(5)	0.3330(5)	1436(63)	923(48)	843(47)	89(45)	77(48)	−239(39)
C(4)	0.2311(7)	0.1934(4)	0.2199(4)	1233(60)	667(40)	881(43)	69(40)	−242(44)	−316(33)
C(5)	0.0021(5)	0.1951(4)	0.1420(4)	755(41)	695(37)	849(40)	87(31)	−111(32)	−289(31)
C(6)	0.2836(7)	0.2619(5)	0.3914(5)	1694(72)	895(48)	1115(54)	60(49)	−505(51)	−352(42)
C(7)	0.3217(7)	0.4042(5)	0.2151(5)	1149(62)	1222(56)	1170(59)	199(48)	332(48)	−320(46)
C(8)	0.1042(5)	0.5322(4)	0.2269(4)	703(41)	787(41)	760(39)	−194(34)	108(33)	−133(32)
C(9)	0.0804(6)	0.4022(5)	0.4089(4)	1101(56)	1162(50)	655(43)	−76(43)	136(40)	22(37)
C(10)	0.2974(6)	0.4668(4)	0.3669(5)	1059(55)	736(42)	1442(60)	−12(38)	−357(45)	−407(40)
O(1)	0.1294(6)	0.4279(4)	0.0151(4)	1992(59)	1254(42)	1150(41)	−258(40)	133(42)	194(33)
O(2)	−0.2010(5)	0.3874(4)	0.1943(4)	1213(44)	1475(45)	1780(50)	336(38)	−166(40)	−926(39)
O(3)	0.0155(6)	0.1129(4)	0.4033(4)	2108(62)	1387(45)	1171(42)	2(43)	464(44)	7(35)
O(4)	0.3232(5)	0.1480(4)	0.2273(3)	1194(41)	1225(39)	1398(41)	350(32)	−341(34)	−644(32)
O(5)	−0.0366(4)	0.1502(3)	0.1028(3)	972(32)	900(29)	1311(35)	22(24)	−266(27)	−601(27)
O(6)	0.3302(7)	0.1836(4)	0.4354(4)	3113(88)	937(37)	1765(53)	542(47)	−1213(57)	−154(36)
O(7)	0.3915(6)	0.4045(5)	0.1607(5)	1906(64)	1779(53)	2003(63)	168(47)	972(53)	−469(46)
O(8)	0.0459(4)	0.6032(3)	0.1788(3)	851(31)	843(29)	1217(36)	−65(25)	−46(27)	55(26)
O(9)	0.0122(5)	0.4063(5)	0.4636(3)	1595(53)	2206(57)	885(37)	15(45)	420(36)	37(37)
O(10)	0.3552(5)	0.5049(4)	0.4007(4)	1400(46)	1069(37)	2390(61)	−126(32)	−786(43)	−629(38)
P(1)	0.30681(12)	0.87511(9)	0.13767(9)	445(9)	530(8)	453(8)	−118(7)	−6(7)	−152(6)
P(2)	0.49832(12)	0.84254(10)	0.27922(9)	487(9)	538(8)	474(8)	−116(7)	−53(7)	−129(7)
N	0.4254(3)	0.8784(3)	0.1847(3)	481(27)	578(25)	471(24)	−113(21)	−32(21)	−115(20)
C(11)	0.2568(4)	0.9969(4)	0.0509(3)	443(32)	551(33)	410(30)	−107(27)	3(27)	−116(24)
C(12)	0.1676(5)	1.0101(4)	−0.0127(4)	651(40)	654(38)	601(36)	−107(31)	−140(33)	−168(32)
C(13)	0.1276(5)	1.1058(5)	−0.0774(4)	707(44)	918(50)	570(38)	−62(41)	−143(33)	−91(37)

C(16)	0.3056(5)	1.0800(4)	0.0491(4)	518(36)	565(37)	654(36)	−83(31)	−63(29)	−129(31)
C(17)	0.3294(5)	0.7853(3)	0.0788(3)	510(37)	525(32)	493(32)	−100(29)	22(29)	−166(25)
C(18)	0.4391(6)	0.7667(5)	0.0430(4)	692(48)	947(46)	919(45)	−253(36)	155(37)	−534(39)
C(19)	0.4608(6)	0.7013(6)	−0.0058(5)	778(52)	1398(62)	1362(63)	−214(49)	291(45)	−944(56)
C(20)	0.3735(8)	0.6525(5)	−0.0173(5)	1203(67)	925(50)	948(51)	−133(50)	154(51)	−588(41)
C(21)	0.2633(7)	0.6710(4)	0.0163(4)	990(56)	791(44)	744(43)	−308(40)	23(40)	−365(37)
C(22)	0.2406(5)	0.7379(4)	0.0648(4)	676(41)	663(35)	606(35)	−219(32)	80(30)	−296(31)
C(23)	0.1888(4)	0.8459(4)	0.2177(3)	468(34)	526(35)	465(31)	−142(29)	−18(26)	−153(29)
C(24)	0.1904(5)	0.7477(4)	0.2780(4)	628(39)	636(40)	663(38)	−190(31)	118(34)	−263(32)
C(25)	0.1074(6)	0.7267(5)	0.3460(4)	897(50)	774(44)	697(43)	−352(42)	217(40)	−223(34)
C(26)	0.0232(6)	0.8039(6)	0.3546(4)	636(45)	1113(56)	730(43)	−376(43)	218(35)	−381(44)
C(27)	0.0189(5)	0.9017(5)	0.2943(5)	565(42)	907(50)	801(44)	−60(36)	103(38)	−368(39)
C(28)	0.1037(5)	0.9224(4)	0.2266(4)	558(37)	663(38)	587(36)	−88(33)	32(33)	−144(29)
C(29)	0.4124(5)	0.8098(4)	0.3828(3)	548(37)	586(36)	451(32)	−178(31)	−74(28)	−112(30)
C(30)	0.4329(6)	0.7141(4)	0.4503(4)	817(46)	712(43)	684(41)	−117(36)	72(38)	−88(35)
C(31)	0.3621(8)	0.6916(5)	0.5271(5)	1228(65)	960(54)	667(47)	−351(52)	164(47)	48(40)
C(32)	0.2721(7)	0.7627(7)	0.5369(5)	1051(61)	1256(65)	628(47)	−418(53)	269(43)	−324(50)
C(33)	0.2514(6)	0.8574(5)	0.4712(5)	860(48)	980(51)	633(42)	−214(40)	118(40)	−414(40)
C(34)	0.3210(5)	0.8821(4)	0.3946(4)	678(41)	669(38)	562(39)	−150(35)	−43(34)	−228(30)
C(35)	0.6082(5)	0.7337(4)	0.2894(3)	492(38)	550(35)	547(33)	−113(28)	−7(29)	−131(27)
C(36)	0.5819(5)	0.6600(4)	0.2598(4)	682(43)	604(39)	982(46)	−19(37)	−144(35)	−265(35)
C(37)	0.6640(7)	0.5742(5)	0.2676(5)	913(56)	700(46)	1169(56)	−29(43)	−113(46)	−375(39)
C(38)	0.7729(6)	0.5614(5)	0.3071(5)	742(53)	729(46)	1105(53)	78(39)	−40(43)	−273(40)
C(39)	0.8008(6)	0.6336(6)	0.3367(5)	570(44)	917(51)	1328(60)	170(43)	−280(40)	−399(46)
C(40)	0.7199(6)	0.7200(5)	0.3281(4)	656(46)	833(46)	909(45)	−81(38)	−145(37)	−355(35)
C(41)	0.5736(4)	0.9432(4)	0.2790(4)	495(34)	536(32)	530(35)	−85(27)	−103(30)	−135(29)
C(42)	0.6229(5)	0.9968(4)	0.1984(4)	768(43)	827(42)	618(40)	−359(37)	39(34)	−256(34)
C(43)	0.6827(6)	1.0734(5)	0.1964(5)	1027(54)	918(49)	804(49)	−424(43)	30(40)	−230(39)
C(44)	0.6909(7)	1.0964(5)	0.2727(6)	1166(61)	942(51)	1091(59)	−610(45)	54(51)	−364(48)
C(45)	0.6414(8)	1.0448(7)	0.3537(5)	1734(83)	1614(74)	902(57)	−954(69)	79(56)	−720(55)
C(46)	0.5816(6)	0.9672(5)	0.3578(4)	1280(61)	1139(52)	569(40)	−672(48)	16(38)	−281(37)
H	0.0750(41)	0.3471(31)	0.2759(29)						

[a] The estimated standard deviations in parentheses for this and all subsequent tables refer to the least significant figure. [b] The form of the anisotropic temperature factors ($\times 10^4$) is $\exp[-2\pi^2(h^2a^{*2}U_{11} + k^2b^{*2}U_{22} + l^2c^{*2}U_{33} + 2hka^*b^*U_{12} + 2hla^*c^*U_{13} + 2klb^*c^*U_{23})]$. The isotropic temperature factor, given by $\exp[-8\pi^2U(\sin^2\theta)/\lambda^2]$, is 0.101 Å^2 for all H atoms.

TABLE 3

POSITIONAL PARAMETERS AND TEMPERATURE FACTORS FOR $[K(crypt\text{-}222)]^+[Mo_2(CO)_{10}(\mu\text{-}H)]^-$ [a]

	Positional parameters			Temperature factors					
Atom	x	y	z	U_{11}	U_{22}	U_{33}	U_{12}	U_{13}	U_{23}
Mo(1)	0.95778(3)	0.74576(2)	0.17449(2)	545(2)	532(2)	546(2)	−52(1)	0(1)	−235(1)
Mo(2)	0.98731(3)	0.85432(3)	0.34258(2)	644(2)	612(2)	508(2)	−8(2)	15(2)	−244(2)
C(1)	1.1492(4)	0.7875(3)	0.1509(2)	667(26)	612(23)	544(21)	24(20)	−13(19)	−210(18)
C(2)	0.9025(4)	0.8708(3)	0.0639(3)	601(24)	657(24)	721(26)	22(20)	20(21)	−269(21)
C(3)	0.7621(5)	0.7259(3)	0.2055(3)	743(30)	726(27)	930(31)	−153(24)	25(25)	−180(23)
C(4)	1.0175(4)	0.6062(3)	0.2746(3)	770(28)	647(26)	823(28)	−76(22)	19(23)	−243(23)
C(5)	0.9689(4)	0.6479(3)	0.1002(3)	730(27)	764(27)	870(29)	20(21)	−149(22)	−378(24)
C(6)	0.8911(5)	0.7173(4)	0.4099(3)	1110(38)	818(31)	837(31)	7(28)	315(27)	−280(26)
C(7)	1.1615(5)	0.7604(3)	0.3570(3)	835(30)	719(26)	717(26)	3(23)	−105(23)	−342(21)
C(8)	1.0733(4)	0.9908(4)	0.2633(3)	592(25)	764(28)	860(29)	33(22)	−20(22)	−252(23)
C(9)	0.8217(4)	0.9569(3)	0.3410(2)	639(25)	761(26)	481(20)	−88(21)	34(19)	−165(19)
C(10)	1.0365(5)	0.8792(3)	0.4525(3)	1163(36)	760(28)	755(28)	312(25)	−248(26)	−329(24)
O(1)	1.2560(3)	0.8130(2)	0.1375(2)	650(18)	949(20)	810(19)	−99(16)	89(15)	−224(15)
O(2)	0.8722(3)	0.9340(3)	−0.0026(2)	995(22)	911(21)	809(20)	138(17)	−105(17)	−141(17)
O(3)	0.6512(3)	0.7227(3)	0.2211(2)	720(22)	1177(27)	1709(35)	−251(20)	207(22)	−330(24)
O(4)	1.0537(3)	0.5245(3)	0.3253(2)	1231(27)	676(19)	1112(24)	−45(18)	−138(20)	−84(18)
O(5)	0.9760(3)	0.5903(3)	0.0565(2)	1180(26)	1191(25)	1342(27)	70(20)	−205(21)	−934(24)
O(6)	0.8368(4)	0.6399(3)	0.4473(3)	1790(38)	962(26)	1469(32)	−367(26)	896(29)	−289(24)
O(7)	1.2614(3)	0.7101(3)	0.3695(2)	905(23)	967(22)	1272(26)	259(19)	−307(20)	−527(20)
O(8)	1.1159(3)	1.0698(3)	0.2172(2)	776(22)	954(24)	1445(30)	−164(18)	77(20)	−2(22)
O(9)	0.7249(3)	1.0172(3)	0.3448(2)	698(19)	1094(22)	755(19)	151(17)	118(15)	−190(16)

N(1)	0.5318(3)	0.1265(2)	0.1074(2)	631(19)	644(19)	503(17)	−4(15)	48(14)	−226(14)
N(2)	0.5251(3)	0.3823(2)	0.3721(2)	925(24)	530(18)	692(21)	103(18)	−149(18)	−263(16)
O(11)	0.4147(2)	0.0469(2)	0.2826(1)	766(16)	591(14)	525(14)	−103(12)	73(12)	−195(12)
O(12)	0.4320(2)	0.1536(2)	0.4132(1)	734(17)	765(17)	647(15)	−124(14)	171(13)	−323(13)
O(13)	0.3967(2)	0.3473(2)	0.0753(2)	784(18)	690(16)	773(17)	163(14)	−239(14)	−323(14)
O(14)	0.3704(3)	0.4542(2)	0.2077(2)	1019(21)	541(15)	760(17)	135(14)	−240(15)	−250(13)
O(15)	0.7739(2)	0.2066(2)	0.1632(2)	653(16)	826(17)	640(16)	−142(14)	116(13)	−209(13)
O(16)	0.7656(3)	0.3446(2)	0.2733(2)	738(19)	776(18)	904(20)	−54(15)	−141(15)	−257(15)
C(11)	0.4517(4)	0.0303(3)	0.1400(2)	811(27)	686(24)	733(25)	−69(21)	8(21)	−401(21)
C(12)	0.4634(4)	−0.0282(3)	0.2378(2)	837(27)	553(22)	725(25)	−134(19)	72(21)	−257(20)
C(13)	0.3950(4)	−0.0065(3)	0.3740(2)	841(28)	742(26)	619(24)	−292(22)	73(21)	−162(21)
C(14)	0.3364(4)	0.0760(4)	0.4152(2)	796(29)	1046(33)	635(24)	−272(26)	175(21)	−320(24)
C(15)	0.3840(4)	0.2319(4)	0.4554(2)	952(32)	887(29)	614(24)	−16(25)	170(22)	−300(22)
C(16)	0.4927(4)	0.3041(3)	0.4594(2)	1044(33)	815(28)	594(24)	72(25)	−31(23)	−369(22)
C(17)	0.4768(4)	0.2001(3)	0.0226(2)	853(29)	826(27)	591(23)	6(23)	−36(21)	−313(21)
C(18)	0.3585(4)	0.2715(3)	0.0337(3)	853(30)	932(30)	751(26)	162(24)	−226(22)	−410(24)
C(19)	0.2900(5)	0.4253(4)	0.0790(3)	1054(36)	915(31)	973(32)	357(28)	−463(27)	−438(27)
C(20)	0.3396(5)	0.5068(3)	0.1171(3)	1136(36)	699(27)	961(32)	332(25)	−353(28)	−326(25)
C(21)	0.4167(5)	0.5286(3)	0.2491(3)	1365(41)	575(26)	1059(35)	307(26)	−346(31)	−344(25)
C(22)	0.4241(5)	0.4747(3)	0.3456(3)	1321(39)	715(27)	879(31)	335(27)	−234(28)	−450(24)
C(23)	0.6706(4)	0.0900(3)	0.0964(2)	786(28)	816(27)	594(22)	71(23)	97(20)	−309(20)
C(24)	0.7689(4)	0.1777(4)	0.0853(3)	669(26)	958(30)	663(25)	27(23)	137(20)	−234(22)
C(25)	0.8687(4)	0.2860(4)	0.1591(3)	614(26)	886(30)	938(32)	−140(23)	130(23)	−133(25)
C(26)	0.8846(4)	0.2960(4)	0.2491(3)	666(30)	886(31)	1113(37)	−209(24)	−49(26)	−257(27)
C(27)	0.7678(4)	0.3475(4)	0.3625(3)	868(32)	852(30)	897(31)	−187(25)	−279(25)	−255(25)
C(28)	0.6561(5)	0.4249(3)	0.3747(3)	1198(38)	568(24)	872(29)	−90(26)	−184(27)	−274(22)
H	0.9233(36)	0.8559(30)	0.2302(23)						

[a] The form of the anisotropic temperature factors ($\times 10^4$) is $\exp[-2\pi^2(h^2a^{*2}U_{11} + k^2b^{*2}U_{22} + l^2c^{*2}U_{33} + 2hka^*b^*U_{12} + 2hla^*c^*U_{13} + 2klb^*c^*U_{23})]$. The isotropic temperature factor, given by $\exp[-8\pi^2U(\sin^2\theta/\lambda^2]$, is 0.076 Å for all H atoms.

TABLE 4

INTERATOMIC DISTANCES (Å) AND BOND ANGLES (DEG) FOR $[(Ph_3P)_2N]^+[Mo_2(CO)_{10}(\mu\text{-}H)]^-$ [a, b]

(A) Distances within the $[Mo_2(CO)_{10}(\mu\text{-}H)]^-$ monoanion

Mo(1)—H	1.76(5)	Mo(2)—H	1.93(5)
Mo(1)—C(1)	2.045(7)	Mo(2)—C(6)	2.027(7)
Mo(1)—C(2)	2.018(8)	Mo(2)—C(7)	1.991(9)
Mo(1)—C(3)	2.005(7)	Mo(2)—C(8)	2.010(6)
Mo(1)—C(4)	2.041(8)	Mo(2)—C(9)	1.979(8)
Mo(1)—C(5)	1.942(8)	Mo(2)—C(10)	1.934(9)
C(1)—O(1)	1.120(9)	C(6)—O(6)	1.129(9)
C(2)—O(2)	1.133(10)	C(7)—O(7)	1.131(12)
C(3)—O(3)	1.138(9)	C(8)—O(8)	1.135(7)
C(4)—O(4)	1.124(10)	C(9)—O(9)	1.133(10)
C(5)—O(5)	1.160(10)	C(10)—O(10)	1.158(12)
Mo(1) ... Mo(2)	3.4219(9)		

(B) Distances within the $[(Ph_3P)_2N]^+$ cation

P—N	1.569(1) av	C—C	1.370(7) av
P—C	1.790(1) av	P···P	2.991

(C) Bond angles within the $[Mo_2(CO)_{10}(\mu\text{-}H)]^-$ monoanion

Mo(1)—H—Mo(2)	136(3)		
H—Mo(1)—C(1)	96(1)	H—Mo(2)—C(6)	91(1)
H—Mo(1)—C(2)	78(1)	H—Mo(2)—C(7)	104(1)
H—Mo(1)—C(3)	82(1)	H—Mo(2)—C(8)	81(1)
H—Mo(1)—C(4)	100(1)	H—Mo(2)—C(9)	76(1)
H—Mo(1)—C(5)	164(1)	H—Mo(2)—C(10)	166(1)
C(1)—Mo(1)—C(2)	92.4(3)	C(6)—Mo(2)—C(7)	89.0(3)
C(1)—Mo(1)—C(3)	175.9(3)	C(6)—Mo(2)—C(8)	172.6(4)
C(1)—Mo(1)—C(4)	88.8(3)	C(6)—Mo(2)—C(9)	91.4(3)
C(1)—Mo(1)—C(5)	90.6(3)	C(6)—Mo(2)—C(10)	91.8(3)
C(2)—Mo(1)—C(3)	91.0(3)	C(7)—Mo(2)—C(8)	91.4(3)
C(2)—Mo(1)—C(4)	178.5(3)	C(7)—Mo(2)—C(9)	179.0(4)
C(2)—Mo(1)—C(5)	87.4(3)	C(7)—Mo(2)—C(10)	89.0(4)
C(3)—Mo(1)—C(4)	87.9(3)	C(8)—Mo(2)—C(9)	88.3(3)
C(3)—Mo(1)—C(5)	92.0(3)	C(8)—Mo(2)—C(10)	95.5(3)
C(4)—Mo(1)—C(5)	93.6(3)	C(9)—Mo(2)—C(10)	90.1(4)
Mo(1)—C(1)—O(1)	178.9(9)	Mo(2)—C(6)—O(6)	179.8(9)
Mo(1)—C(2)—O(2)	175.4(8)	Mo(2)—C(7)—O(7)	179.2(7)
Mo(1)—C(3)—O(3)	178.2(8)	Mo(2)—C(8)—O(8)	176.8(7)
Mo(1)—C(4)—O(4)	178.4(7)	Mo(2)—C(9)—O(9)	177.1(7)
Mo(1)—C(5)—O(5)	178.3(5)	Mo(2)—C(10)—O(10)	179.2(7)

(D) Bond angles within the $[(Ph_3P)_2N]^+$ cation

P(1)—N—P(2)	144.8(2)		
C(11)—P(1)—N	108.8(2)	C(29)—P(2)—N	115.2(2)
C(17)—P(1)—N	111.3(2)	C(35)—P(2)—N	110.6(2)
C(23)—P(1)—N	113.9(2)	C(41)—P(2)—N	108.2(2)
C—P—C	107.5(2) av.	P—C—C	120.4(3) av.
C—C—C	120.0 av.		

[a] The e.s.d.'s given in parentheses for the interatomic separations and bond angles were calculated from the standard errors in the fractional coordinates of the corresponding atomic positions. [b] The e.s.d.'s which are shown in parentheses for the average values are calculated from the formula $\sigma_{\bar{l}} = [\Sigma(l - l_m)^2/(m^2 - m)]^{1/2}$, where m is the number of "equivalent" bonds (or angles), l_m is the value of the mth bond (or angle), and $\bar{l}$ is the mean value.

TABLE 5

INTERATOMIC DISTANCES (Å) AND BOND ANGLES (DEG) FOR $[K(crypt\text{-}222)]^+[Mo_2(CO)_{10}(\mu\text{-}H)]^-$ [a]

(A) Distances within the $[Mo_2(CO)_{10}(\mu\text{-}H)]^-$ monoanion

Mo(1)—H	1.89(4)	Mo(2)—H	1.91(4)
Mo(1)—C(1)	2.026(4)	Mo(2)—C(6)	2.028(5)
Mo(1)—C(2)	2.023(4)	Mo(2)—C(7)	2.026(4)
Mo(1)—C(3)	2.032(5)	Mo(2)—C(8)	2.029(4)
Mo(1)—C(4)	2.039(4)	Mo(2)—C(9)	2.040(4)
Mo(1)—C(5)	1.966(5)	Mo(2)—C(10)	1.956(5)
C(1)—O(1)	1.139(5)	C(6)—O(6)	1.144(6)
C(2)—O(2)	1.142(5)	C(7)—O(7)	1.140(5)
C(3)—O(3)	1.138(6)	C(8)—O(8)	1.144(5)
C(4)—O(4)	1.138(5)	C(9)—O(9)	1.136(5)
C(5)—O(5)	1.158(6)	C(10)—O(10)	1.156(6)
Mo(1) ... Mo(2)	3.4056(5)		

(B) Distances within the $[K(crypt\text{-}222]^+$ cation

K—N(1)	3.023(3)	K—N(2)	3.060(4)		
K—O(11)	2.796(2)	K—O(12)	2.872(3)	K—O(15)	2.803(3)
K—O(12)	2.826(2)	K—O(14)	2.871(3)	K—O(16)	2.827(3)
N(1)—C(11)	1.457(5)	N(1)—C(17)	1.473(4)	N(1)—C(23)	1.465(5)
N(2)—C(16)	1.476(4)	N(2)—C(22)	1.460(5)	N(2)—C(28)	1.464(6)
C(11)—C(12)	1.503(5)	C(13)—C(14)	1.487(6)	C(15)—C(16)	1.488(7)
C(17)—C(18)	1.488(6)	C(19)—C(20)	1.471(7)	C(21)—C(22)	1.475(6)
C(23)—C(24)	1.505(6)	C(25)—C(26)	1.493(7)	C(27)—C(28)	1.493(7)
O(11)—C(12)	1.420(5)	O(13)—C(18)	1.407(6)	O(15)—C(24)	1.405(5)
O(11)—C(13)	1.415(4)	O(13)—C(19)	1.423(5)	O(15)—C(25)	1.418(5)
O(12)—C(14)	1.415(5)	O(14)—C(20)	1.418(5)	O(16)—C(26)	1.412(5)
O(12)—C(15)	1.420(5)	O(14)—C(21)	1.418(6)	O(16)—C(27)	1.435(6)

(C) Bond angles within the $[Mo_2(CO)_{10}(\mu\text{-}H)]^-$ monoanion

Mo(1)—H—Mo(2)	127(2)		
H—Mo(1)—C(1)	91(1)	H—Mo(2)—C(6)	93(1)
H—Mo(1)—C(2)	83(1)	H—Mo(2)—C(7)	103(1)
H—Mo(1)—C(3)	79(1)	H—Mo(2)—C(8)	80(1)
H—Mo(1)—C(4)	104(1)	H—Mo(2)—C(9)	84(1)
H—Mo(1)—C(5)	169(1)	H—Mo(2)—C(10)	169(1)
C(1)—Mo(1)—C(2)	89.1(1)	C(6)—Mo(2)—C(7)	90.0(2)
C(1)—Mo(1)—C(3)	170.6(2)	C(6)—Mo(2)—C(8)	173.8(2)
C(1)—Mo(1)—C(4)	90.7(1)	C(6)—Mo(2)—C(9)	92.1(2)
C(1)—Mo(1)—C(5)	93.6(2)	C(6)—Mo(2)—C(10)	91.5(2)
C(2)—Mo(1)—C(3)	88.9(1)	C(7)—Mo(2)—C(8)	92.1(2)
C(2)—Mo(1)—C(4)	171.9(2)	C(7)—Mo(2)—C(9)	172.2(2)
C(2)—Mo(1)—C(5)	86.8(2)	C(7)—Mo(2)—C(10)	85.4(2)
C(3)—Mo(1)—C(4)	92.6(2)	C(8)—Mo(2)—C(9)	86.6(2)
C(3)—Mo(1)—C(5)	95.4(2)	C(8)—Mo(2)—C(10)	94.5(2)
C(4)—Mo(1)—C(5)	85.1(2)	C(9)—Mo(2)—C(10)	87.0(2)
Mo(1)—C(1)—O(1)	178.7(3)	Mo(2)—C(6)—O(6)	179.5(5)
Mo(1)—C(2)—O(2)	173.5(4)	Mo(2)—C(7)—O(7)	175.5(4)
Mo(1)—C(3)—O(3)	175.2(4)	Mo(2)—C(8)—O(8)	176.8(3)
Mo(1)—C(4)—O(4)	174.4(4)	Mo(2)—C(9)—O(9)	174.4(4)
Mo(1)—C(5)—O(5)	179.7(4)	Mo(2)—C(10)—O(10)	178.4(4)

(D) Bond angles within the $[K(crypt\text{-}222)]^+$ cation

N(1)—K—N(2)	177.7(1)				
N(1)—K—O(11)	59.8(1)	N(1)—K—O(13)	59.5(1)	N(1)—K—O(15)	60.9(1)
N(2)—K—O(12)	60.6(1)	N(2)—K—O(14)	59.1(1)	N(2)—K—O(16)	60.1(1)
N(1)—K—O(12)	120.2(1)	N(1)—K—O(14)	118.6(1)	N(1)—K—O(16)	121.1(1)
N(2)—K—O(11)	120.8(1)	N(2)—K—O(13)	118.2(1)	N(2)—K—O(15)	120.5(1)
O(11)—K—O(12)	60.5(1)	O(12)—K—O(13)	130.6(1)	O(13)—K—O(15)	94.2(1)
O(11)—K—O(13)	95.0(1)	O(12)—K—O(14)	94.6(1)	O(13)—K—O(16)	119.2(1)

TABLE 5 (continued)

(D) Bond angles within the [K(crypt-222)]$^+$ cation

O(11)—K—O(14)	120.3(1)	O(12)—K—O(15)	130.8(1)	O(14)—K—O(15)	129.9(1)
O(11)—K—O(15)	102.4(1)	O(12)—K—O(16)	102.6(1)	O(14)—K—O(16)	93.9(1)
O(11)—K—O(16)	141.4(1)	O(13)—K—O(14)	59.4(1)	O(15)—K—O(16)	60.6(1)
C(11)—N(1)—C(17)	109.4(3)	C(11)—N(1)—C(23)	109.9(3)	C(17)—N(1)—C(23)	110.4(3)
C(16)—N(2)—C(22)	110.6(3)	C(16)—N(2)—C(28)	110.1(3)	C(22)—N(2)—C(28)	109.8(3)
N(1)—C(11)—C(12)	114.4(3)	N(1)—C(17)—C(18)	113.0(3)	N(1)—C(23)—C(24)	114.8(3)
C(11)—C(12)—O(11)	108.3(3)	C(17)—C(18)—O(13)	109.8(3)	C(23)—C(24)—O(15)	109.6(3)
C(12)—O(11)—C(13)	112.5(3)	C(18)—O(13)—C(19)	111.9(3)	C(24)—O(15)—C(25)	112.9(3)
O(11)—C(13)—C(14)	109.3(3)	O(13)—C(19)—C(20)	108.9(4)	O(15)—C(25)—C(26)	109.0(3)
C(13)—C(14)—O(12)	108.9(3)	C(19)—C(20)—O(14)	109.7(3)	C(25)—C(26)—O(16)	109.4(3)
C(14)—O(12)—C(15)	111.6(3)	C(20—O(14)—C(21)	112.8(3)	C(26)—O(16)—C(27)	112.9(3)
O(12)—C(15)—C(16)	109.3(3)	O(14)—C(21)—C(22)	110.2(3)	O(16)—C(27)—C(28)	109.0(3)
C(15)—C(16)—N(2)	112.9(3)	C(21)—C(22)—N(2)	113.1(4)	C(27)—C(28)—N(2)	112.7(4)

[a] The corresponding bonding parameters for the hydrogen atoms in the [K(crypt-222)]$^+$ cation are provided in the supplementary material.

The "goodness-fo-fit" parameter, σ_1, was calculated from $\sigma_1 = [\Sigma\omega_i|F_o^2 - F_c^2|/(n-p)]^{1/2}$, where n is the number of observations and p is the number of parameters varied. A final Fourier difference map in each case revealed no regions of residual electron density greater than 0.3 $e^-/Å^3$ and thereby verified the correctness of the structural analyses. The scattering factors utilized in all structure factor calculations were those of Cromer and Mann [13] for the non-hydrogen atoms and those of Stewart et al. [14] for the hydrogen atoms. Corrections were included for anomalous dispersion effects [15] for the non-hydrogen atoms.

The positional and thermal parameters obtained from the last least-squares refinement cycles are presented in Tables 2 and 3 for $[(Ph_3P)_2N]^+[Mo_2(CO)_{10}(\mu\text{-H})]^-$ and $[K(crypt\text{-}222)]^+[Mo_2(CO)_{10}(\mu\text{-H})]^-$, respectively. The e.s.d.'s provided for the positional parameters of the bridging H atom in each case were calculated during a full-matrix refinement performed on only the anion just prior to the final refinement cycle. The corresponding interatomic distances and bond angles, calculated from the estimated standard errors of the fractional coordinates, are provided in Tables 4 and 5. The atom numbering scheme for each salt is similar to that used for the respective Cr analogue [2b,3]. Least-squares planes defined by specific atoms in the $[Mo_2(CO)_{10}(\mu\text{-H})]^-$ anion and their dihedral angles have been calculated and are included in the deposited material. * The computer programs which were employed to perform the necessary computations have been described elsewhere [16].

* A table of the hydrogen positional parameters for the $[(Ph_3P)_2N]^+$ and $[K(crypt\text{-}222)]^+$ cations, a table of bond distances and angles for the hydrogen atoms in the $[K(crypt\text{-}222)]^+$ cation, a complete table of the bond distances in the $[(Ph_3P)_2N]^+$ cation, a table summarizing the least-squares planes calculation for the $[Mo_2(CO)_{10}(\mu\text{-H})]^-$ anion of each salt, a table of torsional angles in the $[K(crypt\text{-}222)]^+$ cation, and the corresponding structure factor tables have been deposited as NAPS Document No. 03764 (39 pages). Order from ASIS/NAPS, c/o Microfiche Publications, P.O. Box 3513, Grand Central Station, New York, NY 10017. Remit in advance, in U.S. funds only, $ 9.75 for photocopies or $ 3.00 for microfiche. Outside the U.S.A. and Canada add postage of $ 3.00 for photocopy and $ 1.00 for microfiche.

Results and discussion

General description of the crystal and molecular structures

The crystal structures of $[(Ph_3P)_2N]^+[Mo_2(CO)_{10}(\mu\text{-}H)]^-$ and $[K(crypt\text{-}222)]^+[Mo_2(CO)_{10}(\mu\text{-}H)]^-$ are depicted stereographically in Figs. 1 and 2, which show the arrangement of the two cations and two anions in their respective triclinic unit cells. Since the structures of the ions are not constrained by crystallographically-imposed symmetry, the crystallographic asymmetric unit in each case contains one cation and one anion. The interionic contracts to not suggest the presence of any unusual interactions among the ions. For $[K(crypt\text{-}222)]^+[Mo_2(CO)_{10}(\mu\text{-}H)]^-$ this result is a bit surprising since our structural investigation of $[K(crypt\text{-}222)]^+[Cr_2(CO)_{10}(\mu\text{-}H)]^-$ [3] has shown that the K^+ ion interacts with an O atom of one of the carbonyl groups. The relatively close K···O separation of 2.966(3) Å, which is nearly equal to the sum of the corresponding ionic radii of ca. 2.9 Å, suggests the presence of an appreciable cation—anion interaction. Although this interaction does not noticeably perturb the local C_{4v} symmetry of the $Cr(CO)_5$ fragment, it leads to a twisting distortion of the metal carbonyl framework from an eclipsed configuration [3]. By comparison the shortest K···O interionic separation in the molybdenum analogue is 3.444(3) Å.

The molecular configuration of the $[Mo_2(CO)_{10}(\mu\text{-}H)]^-$ anion closely conforms to that previously observed for the analogous tungsten salts. For $[Et_4N]^+[W_2(CO)_{10}(\mu\text{-}H)]^-$ a linear, eclipsed metal carbonyl configuration is observed, whereas for the corresponding $[(Ph_3P)_2N]^+$ salt, a bent, staggered carbonyl structure for the anion is found [4]. Although a complete structural analysis of $[Et_4N]^+[Mo_2(CO)_{10}(\mu\text{-}H)]^-$ was not undertaken, the similar magnitude of the lattice parameters for the Mo and W salts is reasonable evidence to conclude that they are isomorphous. For the $[(Ph_3P)_2N]^+$ and $[K(crypt\text{-}222)]^+$ salts our structural determinations have shown that the appreciably bent, staggered carbonyl configuration is preferred by the $[Mo_2(CO)_{10}(\mu\text{-}H)]^-$ anion.

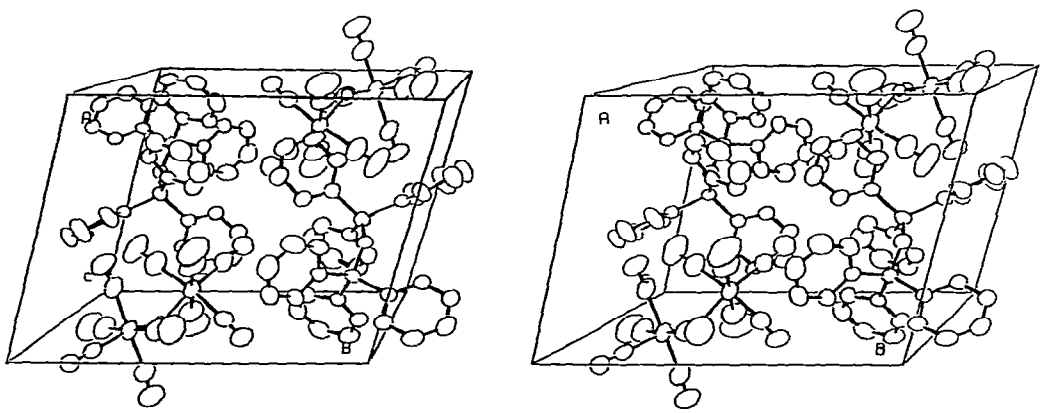

Fig. 1. Stereographic view of the arrangement of two $[Mo_2(CO)_{10}(\mu\text{-}H)]^-$ anions and two $[(Ph_3P)_2N]^+$ cations in the triclinic unit cell of $P\bar{1}$ symmetry. The thermal ellipsoids for the non-hydrogen atoms were scaled to enclose 40% probability.

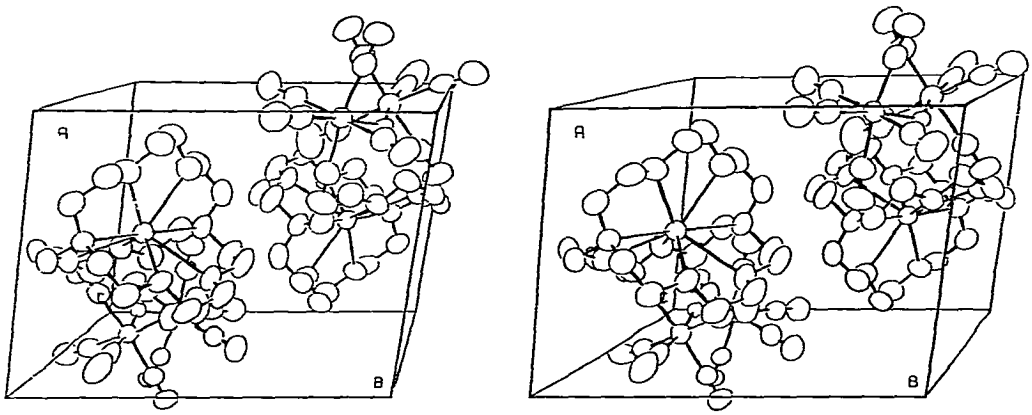

Fig. 2. Stereographic view of the corresponding unit cell contents of $[K(crypt\text{-}222)]^+[Mo_2(CO)_{10}(\mu\text{-}H)]^-$. The thermal ellipsoids are scaled to enclose 50% probability.

The structure of the $[(Ph_3P)_2N]^+$ cation adopts the usual bent P—N—P configuration, with P—N distances of 1.570(4) and 1.568(4) Å and a P—N—P angle of 144.8(2)°. The six independent phenyl rings are each planar within experimental error and a nearly tetrahedral geometry is retained about each phosphorus atom.

The conformational structure of the $[K(crypt\text{-}222)]^+$ cation is in accord with that observed for [K(crypt-222)]I [17] in which the K^+ ion is surrounded by the cryptate molecule and coordinated to six O atom and two N atom donors. The normal "in-in" nitrogen configuration is found with N(1) and N(2) displaced 0.478(4) and 0.472(4) Å from C(11), C(17), C(23) and C(16), C(22), C(28) planes, respectively, toward the central K^+ ion. The K—N distances are 3.023(3) and 3.060(4) Å with a nearly linear N—K—N bond angle of 177.7(1)°. The six K—O distances range from 2.769(2) to 2.872(3) Å. The geometry of the six oxygen atoms of the cation resembles closely a trigonal prism. The twist angle, defined as the torsional angle between two O—CNT vectors, where CNT is the centroid of the respective triangular face of the prism and O is one of the pair of O atoms which share an edge of the prism, is 6.3° (av) compared to 10.8° (av) for $[K(crypt\text{-}222)]^+[Cr_2(CO)_{10}(\mu\text{-}H)]^-$ [3] and 22.5° (av) for [K(crypt-222)] [17]. The magnitude of this torsional angle is related inversely to the N···N separation which is ca. 6.08, 5.98, and 5.75 Å, respectively, for these $[K(crypt\text{-}222)]^+$ salts. As the cryptate ion is elongated, the triangular faces of the prism approach a more nearly eclipsed alignment.

Molecular configuration of the $[Mo_2(CO)_{10}(\mu\text{-}H)]^-$ anions

From our structural analysis the molecular structure of the $[Mo_2(CO)_{10}(\mu\text{-}H)]^-$ anion is influenced strongly by the choice of the counter cation. For the three salts which we have examined, the $[Mo_2(CO)_{10}(\mu\text{-}H)]^-$ anion can adopt either a nearly eclipsed configuration as presumed for the $[Et_4N]^+$ salt or an appreciably bent metal carbonyl arrangement for the fully characterized $[(Ph_3P)_2N]^+$ and $[K(crypt\text{-}222)]^+$ salts. This observed variation in the structure of the $[Mo_2(CO)_{10}(\mu\text{-}H)]^-$ anion is reminiscent of that observed for the

$[(Ph_3P)_2N]^+$ cation with the degree of bending of the P—N—P bond angle (i.e., 135—180°) dependent upon in this case the counter anion [18].

Perspective views of the anion's configuration found for each of these two salts are shown in Fig. 3 with the atom labeling scheme. A comparison of the appropriate X-ray-determined structural parameters indicate that their overall configurations are reasonably similar. A pseudo-octahedral geometry is maintained about each metal center. The greater π-acceptor ability of the axial CO ligand *trans* to the bridging H atom is reflected by the 0.05—0.09 Å shorter Mo—$C_{(ax)}$ distance and the 0.02—0.03 Å longer $C_{(ax)}$—$O_{(ax)}$ distance compared to the corresponding equatorial carbonyl distances. The staggered carbonyl arrangement is confirmed by the ca. 45° dihedral angles between appropriate pairs of planes passing through two *trans* equatorial carbonyl carbons, the axial carbonyl carbon, and the Mo atom of each $Mo(CO)_5$ moiety.

The principal difference between these two configurations is the dihedral angle between the two equatorial planes in the anion. For the $[(Ph_3P)_2N]^+$ salt the dihedral angle is 15.4° compared to a substantially larger value of 29.9° for the [K(crypt-222)]$^+$ salt. The corresponding angles of intersection between the two Mo—$CO_{(ax)}$ vectors are 165.7(3) and 148.2(2)°, respectively, and reflect the

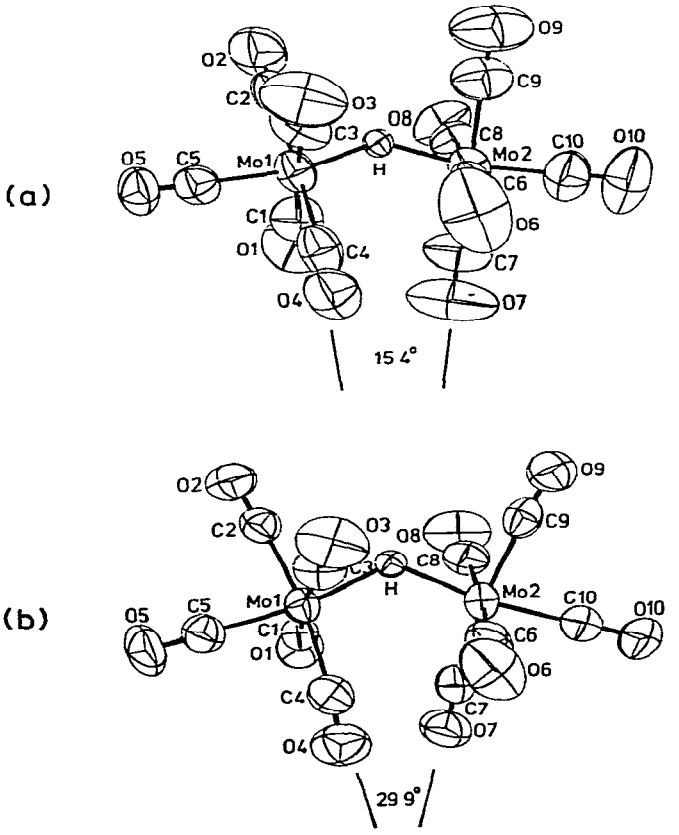

Fig. 3. Prespective views of the $[Mo_2(CO)_{10}(\mu\text{-H})]^-$ anion for the (a) $[(Ph_3P)_2N]^+$ and (b) [K(crypt-222)]$^+$ salts. The dihedral angles between the two planes containing the equatorial carbonyl carbons are 15.4 and 29.9°, respectively.

greater bending of the Mo—H—Mo bond in the metal carbonyl framework of the $[K(crypt\text{-}222)]^+$ salt. This bending reduces the Mo···Mo separation of the three-center, two-electron Mo—H—Mo bond from 3.4219(9) to 3.4056(5) Å and produces a greater displacement of the equatorial carbonyl atoms out of their equatorial plane. For $[(Ph_3P)_2N]^+[Mo_2(CO)_{10}(\mu\text{-}H)]^-$ the equatorial carbonyl groups of the anion are for the most part displaced toward the bridging hydride. In contrast, for $[K(crypt\text{-}222)]^+[Mo_2(CO)_{10}(\mu\text{-}H)]^-$ an alternating pattern is established where carbonyls 1, 3, 6 and 8 are bent toward while carbonyls 2, 4, 7, and 9 are bent away from the hydride. This variation associated with the orientation of the equatorial carbonyls in the $[K(crypt\text{-}222)]^+$ salt probably helps to relieve some of the increased steric repulsion between the two $Mo(CO)_5$ units that accompanies the reduction of the Mo—H—Mo angle. From this comparison of these various configurations of the $[Mo_2(CO)_{10}(\mu\text{-}H)]^-$ anion, it is apparent that lattice effects have a significant influence upon the degree of bending associated with the anion's solid-state geometry.

With this in mind, let us consider the consequences of phosphine substitution upon the molecular framework of the $[Mo_2(CO)_{10}(\mu\text{-}H)]^-$ anion. From the reactions of PPh_3 and excess $PMePh_2$ with $[Mo_2(CO)_{10}(\mu\text{-}H)]^-$, Darensbourg, Atwood and co-workers [6,7] have isolated a monophosphine-substituted hydride, $[Et_4N]^+[Mo_2(CO)_9(PPh_3)(\mu\text{-}H)]^-$ and a diphosphine-substituted hydride, $[Et_4N]^+[Mo_2(CO)_8(PMePh_2)_2(\mu\text{-}H)]^-$, respectively. Their subsequent structure determinations of these salts have shown that both anions prefer a bent, staggered metal carbonyl configuration with the phosphine substituent(s) *cis* to the hydride bridge. In these phosphine derivatives a similar difference in the degree of bending associated with the molecular framework is observed. For the monosubstituted anion the angle of interaction between the two $M—CO_{(ax)}$ vectors is 163° (compared to 166° in $[(Ph_3P)_2N]^+[Mo_2(CO)_{10}(\mu\text{-}H)]^-$), whereas for the disubstituted anion it is 148° (identical to that in $[K(crypt\text{-}222)]^+$-$[Mo_2(CO)_{10}(\mu\text{-}H)]^-$). The greater bending of the disubstituted anion is similarly accompanied by a ca. 0.03 Å decrease in the Mo···Mo separation. Based upon steric factors one can reasonably understand why *cis* placement of the two $PMePh_2$ substituents in $[Mo_2(CO)_8(PMePh_2)_2(\mu\text{-}H)]^-$ anion produces a more pronounced bending of the Mo—H—Mo bond. However, from our structural data, it becomes apparent that the same alteration of the metal carbonyl framework and its Mo···Mo separation can be accomplished by use of a different counter cation. The replacement of $[Et_4N]^+$ by $[(Ph_3P)_2N]^+$ and then by $[K(crypt\text{-}222)]^+$ has been shown to produce a continual increase in the dihedral angle between the equatorial planes. This result reflects the inherent flexible nature of the Mo—H—Mo bond. Therefore, from the structural data available for these various salts of the $[Mo_2(CO)_{10}(\mu\text{-}H)]^-$ anion and its phosphine-substituted derivatives, one must conclude that a delicate balance exists between steric, electronic, and lattice effects which in each case collectively control the ultimate configuration of these hydride complexes in the crystal lattice.

Acknowledgements

Computer time for the X-ray diffraction data analyses was provided by the West Virginia Network for Educational Telecomputing. The authors would like to thank S. Bart Jones for measuring the NMR spectra.

References

1 (a) L.B. Handy, P.M. Treichel, L.F. Dahl and R.G. Hayter, J. Amer. Chem. Soc., 88 (1966) 366; (b) L.B. Handy, J.K. Ruff and L.F. Dahl, ibid., 92 (1970) 7312.
2 (a) J. Roziere, J.M. Williams, R.P. Stewart, Jr., J.L. Petersen and L.F. Dahl, J. Amer. Chem. Soc., 99 (1977) 4497; (b) J.L. Petersen, P.L. Johnson, J. O'Connor, L.F. Dahl and J.M. Williams, Inorg. Chem., 17 (1978) 3460; (c) J.L. Petersen, R.K. Brown, J.M. Williams and R.K. McMullan, Inorg. Chem., 18 (1979) 3493.
3 J.L. Petersen, R.K. Brown and J.M. Williams, Inorg. Chem., 20 (1981) 158.
4 R.D. Wilson, S.A. Graham and R. Bau, J. Organometal. Chem., 91 (1975) C49.
5 (a) R. Bau, R.G. Teller, S.W. Kirtley and T.F. Koetzle, Accts. Chem. Res., 12 (1979) 176; (b) D.W. Hart, R. Bau and T.F. Koetzle, to be published.
6 M.Y. Darensbourg, J.L. Atwood, R.R. Burch, Jr., W.E. Hunter and N. Walker, J. Amer. Chem. Soc., 101 (1979) 2631.
7 M.Y. Darensbourg, J.L. Atwood, W.E. Hunter and R.R. Burch, Jr., J. Amer. Chem. Soc., 102 (1980) 3290.
8 R.G. Hayter, J. Amer. Chem. Soc., 88 (1966) 4376.
9 R.A. Jacobson, J. Appl. Crystallogr., 9 (1976) 115.
10 W.R. Busing in F.R. Ahmed (Ed.), Crystallographic Computing, Munksgaard, Copenhagen, 1970, 319.
11 J.C. Calabrese, MIRAGE, Ph.D. Thesis (Appendix III), University of Wisconsin, Madison, 1971.
12 J.P. Declerq, D. Germain, P. Main and M.M. Woolfson, Acta Crystallogr., A, 29 (1973) 231.
13 D.T. Cromer and J. Mann, Acta Crystallogr., A, 24 (1968) 321.
14 R.F. Stewart, E.R. Davidson and W.T. Simpson, J. Chem. Phys., 42 (1965) 3175.
15 D.T. Cromer and D. Liberman, J. Chem. Phys., 53 (1970) 1891.
16 J.L. Petersen, J. Organometal. Chem., 166 (1979) 179.
17 P.D. Moras, B. Metz and R. Weiss, Acta Crystallogr., B, 29 (1973) 383.
18 R.D. Wilson and R. Bau, J. Amer. Chem. Soc., 96 (1974) 7601 and references cited therein.